

---

Masters Theses

Student Theses and Dissertations

---

Summer 2024

## Human Arm Stiffness Estimation Method Developed for overground Physical Interaction Experiments: Experimental Validation and Perspectives for Future Applications

Tarani Kanth Kamma  
*Missouri University of Science and Technology*

Follow this and additional works at: [https://scholarsmine.mst.edu/masters\\_theses](https://scholarsmine.mst.edu/masters_theses)



Part of the [Mechanical Engineering Commons](#)

Department:

---

### Recommended Citation

Kamma, Tarani Kanth, "Human Arm Stiffness Estimation Method Developed for overground Physical Interaction Experiments: Experimental Validation and Perspectives for Future Applications" (2024). *Masters Theses*. 8212.  
[https://scholarsmine.mst.edu/masters\\_theses/8212](https://scholarsmine.mst.edu/masters_theses/8212)

This thesis is brought to you by Scholars' Mine, a service of the Missouri S&T Library and Learning Resources. This work is protected by U. S. Copyright Law. Unauthorized use including reproduction for redistribution requires the permission of the copyright holder. For more information, please contact [scholarsmine@mst.edu](mailto:scholarsmine@mst.edu).

HUMAN ARM STIFFNESS ESTIMATION METHOD DEVELOPED FOR  
OVERGROUND PHYSICAL INTERACTION EXPERIMENTS: EXPERIMENTAL  
VALIDATION AND PERSPECTIVES FOR FUTURE APPLICATIONS

by

TARANI KANTH KAMMA

A THESIS

Presented to the Graduate Faculty of the  
MISSOURI UNIVERSITY OF SCIENCE AND TECHNOLOGY

In Partial Fulfillment of the Requirements for the Degree

MASTER OF SCIENCE

in

MECHANICAL ENGINEERING

2024

Approved by:

Yun Seong Song, Advisor  
Devin Burns  
K. Krishnamurthy

© 2024

TARANI KANTH KAMMA

All Rights Reserved

## **PUBLICATION THESIS OPTION**

This thesis consists of the following article, formatted in the style used by the Missouri University of Science and Technology:

Paper I: Pages 4-18 have been submitted to the 45<sup>th</sup> Annual International Conference of the IEEE Engineering in Medicine and Biology Society, on July 26<sup>th</sup>, 2023.

## ABSTRACT

To build a physically interactive robot for overground applications, it is crucial to first understand the biomechanics of humans underlying overground physical human-robot interaction (pHRI) tasks. Estimating human arm stiffness during overground interactive tasks is a promising first step toward this goal. For this, an arm stiffness estimation technique was developed in our previous works that consider the unique challenges involving overground pHRI, such as the need to estimate the arm stiffness from a short duration of data with fewer repetitions. In this work, our stiffness estimation method is further validated with a passive spring setup with known stiffness values, as well as with a human experiment setup that resembles the widely used seated reaching tasks. Results show that our method can estimate the passive spring stiffness within 0.5% of error. We were also able to verify our stiffness values with that of well-known literature, and our method of measurement was able to distinguish between static and dynamic conditions. Also detailed analysis was presented on data extraction from previous art for making meaningful comparisons. To know the learning effect, among our subjects over the series of trials we present a detailed analysis of the stiffness data to see if it was significant. Further to demonstrate a possible experimental condition with the Ophrie robot, we present a Force -Velocity and Force-Acceleration relationship that can be used to determine the roles of dyads in a pHRI protocol.

## ACKNOWLEDGMENTS

This research was a without a question a big milestone in my professional accomplishments, and there are some important people that helped me accomplish this. Firstly, I would like to thank Missouri University of Science and Technology for accepting me to their institution and allowing me to study here. The school has provided me with so many opportunities to learn and explore new things while also allowing me to hone my skills. Secondly, I would like to thank my advisor Dr. Yun Seong Song for funding my research and education and being a wonderful advisor. His efforts and concern toward me have trained me to think in the lines of a researcher, and I have learnt how to develop a potential experimental protocol. This was possible only because of his advising and guidance. Thirdly, I would like to thank Dr. Devin Burns for being a part of me thesis committee and helping us with the research efforts. He has been very instrumental in providing the direction of research and the data analysis part of it. I enjoyed the discussions we had over data analysis. This has given me tremendous insights on how to obtain data from subjects and how to process them. I also would like to thank Dr. Krishnamurthy for being a part of my thesis committee. He has provided me with many tools for conducting research during my journey at the school. Finally, I take this opportunity to thank Sambad Regmi for helping with the conduct of experiements. His deep and vast knowledge of the Ophrie Robot has helped me run the experiment trails. His guidance and help in the lab deserve great appreciation.

## TABLE OF CONTENTS

	Page
PUBLICATION THESIS OPTION.....	iii
ABSTRACT.....	iv
ACKNOWLEDGMENTS .....	iv
LIST OF ILLUSTRATIONS .....	ix
LIST OF TABLES .....	xi
 SECTION	
1. INTRODUCTION.....	1
1.1. ARM STIFFNESS MEAUREMENT.....	1
1.2. EXECUTOR-CONDUCTOR RELATIONSHIP IN pHRI INTERACTION EXPERIEMNTS .....	3
 PAPER	
I. VALIDATION OF HUMAN ARM STIFFNESS ESTIMATION METHOD DEVELOPED FOR OVERGROUND PHYSICAL INTERACTION EXPERIMENTS .....	1
ABSTRACT.....	4
1. INTRODUCTION.....	5
2. METHODS.....	6
2.1. PASSIVE SPRING EXPERIMENT.....	8
2.2. SEATED HUMAN EXPERIMENT.....	9
2.3. DATA ANALYSIS.....	11
3. RESULTS.....	11

3.1. RESULTS FROM PASSIVE SPRING EXPERIMENTS.....	11
3.2. RESULTS FROM SEATED HUMAN EXPERIMENTS.....	12
4. DISCUSSION .....	13
5. CONCLUSION .....	17
REFERENCES.....	17

## SECTION

2. FURTHER DISCUSSION AND DATA ANALYSIS.....	19
2.1. DATA EXTRACTION FROM PRIOR ART.....	19
2.2. DATA ANALYSIS FOR LEARNING EFFECT.....	23
2.2.1. Early Versus Late Trials.....	23
2.2.2. Early Versus Middle Trials. ....	23
2.2.3. Static Trials.....	24
2.2.4. Dyanmic Trials. ....	25
3. FORCE-VELOCITY AND FORCE-ACCELERATION ANALYSIS .....	27
3.1. FORCE, VELOCITY, ACCELERATION CONVENTION.....	27
3.2. EXECUTORSHIP: FORCE-VELOCITY RELATION .....	28
3.3. CONDUCTORSHIP: FORCE-ACCELARATION RELATION .....	29
3.4. OPHRIE AS A CONDUCTOR-EXECUTOR .....	30
3.4.1.Ophrie Handle Acting As A Background Stiffness. ....	30
3.4.2. Ophrie Handle Acting As A Damper.. ....	31
3.4.3. Ophrie Handle Acting As An Inertial Mass.. ....	34
3.5. DISCUSSION AND ANALYSIS .....	35

4. CONCLUSIONS .....	37
APPENDICES	
A. PARTICIPANT'S INFORMATION .....	38
B. SEQUENTIAL INSTRUCTIONS FOR THE EXPERIMENTER.....	40
C. MATLAB CODE FOR DATA PROCESSING .....	43
BIBLIOGRAPHY .....	48
VITA .....	50

## LIST OF ILLUSTRATIONS

PAPER I	Page
Figure 1. Passive spring setup: front view (Left) and top view (Right). .....	8
Figure 2. Photo of Ophrie (Left) and the human experiment setup (Right). .....	9
Figure 3. Linear regression of stiffness measurement from spring experiments using 2, 3, and 4-spring configurations. ....	14
Figure 4. Arm stiffness estimation for each subject (A) static condition (B) dynamic condition.....	14
Figure 5. Sensitivity of arm stiffness estimation method to reveal differences between (A)experimental conditions and (B) learning effect between early and late trials within static trials .....	15
Figure 6. Arm stiffness comparison between this work, Gomi& Kawato [8], and Mussa-Ivaldi et al. [9] (A) static condition, (B)dynamic condition. ....	15
 SECTION	
Figure 2.1. Arm stiffness ellipses reported in [10] for static condition. ....	20
Figure 2.2. Pixel representation of the 50N/m reference used in [10] to compute the stiffnesses of the 3 subjects used in their study. ....	21
Figure 2.3. Pixel representation of the stiffnesses of the 3 subjects used in the study of [10].....	22
Figure 3.1. Force, displacement, velocity and acceleration depiction in a dyad interaction. ....	28
Figure 3.2. Schematic of the Human Ophrie set-up for executor conductor role determination in different conditions.....	30
Figure 3.3. The variation of force, displacement, velocity, and acceleration on Ophrie handle acting as a background stiffness. (Right) The executor and conductor roles exhibited by human subject and Ophrie handle during background stiffness condition.. ....	32

Figure 3.4. The variation of force, displacement, velocity, and acceleration on Ophrie handle acting as a damper. (Right) The executor and conductor roles exhibited by Human subject and Ophrie handle during damping condition.. 33

Figure 3.5. The variation of force, displacement, velocity, and acceleration on Ophrie handle acting as an Intertial mass. (Right) The executor and conductor Roles exhibited by Human subject and Ophrie handle during Inertial Mass condition.. ..... 35

## LIST OF TABLES

SECTION	Page
Table 2.1. ANOVA and Effects Summary for Early Versus Late Trials .....	25
Table 2.2. ANOVA and Effects Summary for Early Versus Middle Trials .....	26
Table 2.3. ANOVA and Effects Summary for Static Trials. ....	26
Table 2.4. ANOVA and Effects Summary for Dynamic Trials.....	26
Table 3.1. Executorship Determination in Background Stiffness.....	31
Table 3.2. Conductorship Determination in Background Stiffness. ....	31
Table 3.3. Executorship Determination in Damping Condition. ....	33
Table 3.4. Conductorship Determination in Damping Condition.....	33
Table 3.5. Executorship Determination in Inertial Mass Condition. ....	34
Table 3.6. Conductorship Determination in Inertial Mass Condition.....	34

# 1. INTRODUCTION

## 1.1. ARM STIFFNESS MEASUREMENT

To physically interact with humans, robots need to be equipped with functionalities that make them more dependable and safer [1,2,3]. To make Physical Human Robot Interaction (pHRI) not only safe but more convenient and comfortable for humans, it is essential to first understand the human motor control strategy during overground physical human-robot interaction (pHRI) [4-8]. A promising approach for studying human motor control is to analyze the mechanical impedance of human arms - particularly, the stiffness component [9-10]. It not only helps understand the human motor control strategy but also helps in the development of a stable interaction platform [11]. Arm stiffness was studied extensively to understand the motor control strategy during reaching movements or arm pose selection [8-10]. However, in these prior works the subjects were in seated condition only, allowing for long duration (1.5 seconds or more) of the external perturbation as well as a large number of trials (40 or more per arm configuration). When interacting with a robot in a overground setting, it is desirable to have shorter duration of perturbation and less number of trials.

More recently, arm stiffness was studied during overground tasks that are more similar to the foreseen applications of pHRI [5, 14]. These experiments involved a novel interactive robot Ophrie (an acronym for over-ground physical human-robot Interaction experiments) and a new stiffness measurement technique suitable for overground pHRI experiments [5, 11, 12]. Due to the frequent modulation of arm movements and the increased complexity of overground experiments, only a short period (500 ms or less)

was available for data collection for arm stiffness measurements. The arm stiffness values measured through this method were within the range of those in prior work [10-12]. However, to understand the proper use of this method, such as the variability, accuracy, or length of the data used for stiffness measurements, further investigations were warranted. To this end this work presents the validation of the single-perturbation, non-linear regression method of measuring human arm stiffness for the purpose of future overground pHRI applications. Since no prior art reported arm stiffness measurements during overground pHRI, we compared our method with prior art with seated pHRI [10,11]. First, the method was used to estimate the stiffness of passive mechanical springs with known stiffness values. Then, human experiments with tasks similar to [10] and [11] were conducted to compare the arm stiffness values obtained with different methods.

To validate our stiffness estimation method, we had to compare our compare results with that of prior art [10,11]. However [10] has not directly reported the numerical values of stiffness in their work but rather they made a graphical representation of the stiffness ellipses of their subjects in static condition involving 5 different postures. To make meaningful comparisons we had to extract numerical values of stiffnesses of their subjects from these ellipses by identifying the posture that was most relevant to our arm condition. This method of extraction was discussed in detail in section 2.1 of this work to obtain the numerical values.

One important factor in most pHRI experiments is learning effects over the trials. And in this work, we have conducted a high number of trials to understand the modulation of arm stiffness over the trials, and between static and dynamic arm conditions. To Understand if learning effect was significant, we had to group our trials

into different categories and perform statistical analysis across them to see if and how significant the learning effect was. Section 2.2 of this work presents the relevant analysis to know if the learning effect was significant.

## **1.2. EXECUTOR-CONDUCTOR RELATIONSHIP IN pHRI INTERACTION EXPERIMENTS**

One interesting discussion regarding physical interaction between two entities (pHHI or pHRI) is the existence of the roles and how they affect the dynamics of the interaction. In pHHI, conductorship-executorship role assignment was proposed [17] which could contextualize the role assignments between two active humans. On the other hand, such role assignment for pHRI may not act the same way as in pHHI. Moreover, if the robot was programmed to be passive (ex. OPHRIE), then, according to the definition of conductor and executor in [17], the passive robot should not take any active roles. Hence, we explored the applicability of the role assignments in pHHI [17] in our specific pHRI experiments where OPHRIE can be a passive inertia, damping, or spring. In [17], they used a Force-Velocity and Force-Acceleration relationship to determine the roles of executor and conductor. Mathematical expressions were presented in each of these three cases to demonstrate the changes in velocity and acceleration as the handle moved to and from the mean position. The results of executorship and conductorship assignment in each case are computed per the convention discussed in [17]. The implications of how these results would pave way for development of future robots for overground physical interactions has been discussed. Further the limitations of directly applying the convention mentioned in [17] to a pHRI thought experiment have been mentioned.

## **PAPER**

### **I. VALIDATION OF THE HUMAN ARM STIFFNESS ESTIMATION METHOD DEVELOPED FOR OVERGROUND PHYSICAL INTERACTION EXPERIMENTS**

#### **ABSTRACT**

To build a physically interactive robot for overground applications, it is crucial to first understand the biomechanics of humans underlying overground physical human-robot interaction (pHRI) tasks. Estimating human arm stiffness during overground interactive tasks is a promising first step toward this goal. For this, an arm stiffness estimation technique was developed in our previous works that consider the unique challenges involving overground pHRI, such as the need to estimate the arm stiffness from a short duration of data with fewer repetitions. In this work, our stiffness estimation method is further validated with a passive spring setup with known stiffness values, as well as with a human experiment setup that resembles the widely used seated reaching tasks. Results show that our method can estimate the passive spring stiffness within 0.5% of error. We also show that the human arm stiffness measured through our method is comparable to those reported in well-known literature. In addition, our method was able to discern experimental conditions such as early vs. late trials or differences in arm movement conditions. Implications of these results are discussed further.

## 1. INTRODUCTION

Future applications of robots are expected to involve physical interactions with humans in an overground setting, such as in human-robot collaborations in manufacturing or movement assistance for patients in healthcare settings [1, 2]. To build mobile robots that can seamlessly interact with humans in such scenarios where humans and robots can synchronously walk with each other, it is essential to first understand the human motor control strategy during overground physical human-robot interaction (pHRI) [3-7]. This is a crucial step in developing overground robots that can effectively, intuitively, and safely interact with humans through physical interactions.

A promising approach for studying human motor control is to analyze the mechanical impedance of human arms - particularly, the stiffness component [8-10]. Arm stiffness was studied extensively to understand the motor control strategy during reaching movements or arm pose selection [8-10]. These prior works studied arm stiffness in tasks where both the robot and the human body are stationary except for their arms. This allowed using stiffness measurement techniques that involve a long duration (1.5 seconds or more) of the external perturbation that is necessary for measuring the stiffness, as well as a large number of trials (40 or more per arm configuration).

More recently, arm stiffness was studied during overground tasks that are more similar to the foreseen applications of pHRI [5, 11]. These experiments involved a

novel interactive robot Ophrie (an acronym for over-ground physical human-robot Interaction experiments) and a new stiffness measurement technique suitable for overground pHRI experiments [5, 11, 12]. Due to the frequent modulation of arm movements and the increased complexity of overground experiments, only a short period (500 ms or less) was available for data collection for arm stiffness measurements. The arm stiffness values measured through this method were within the range of those in prior work [8- 10]. However, further investigations were warranted to understand the proper use of this method, such as the variability, accuracy, or length of the data used for stiffness measurements.

To this end, this work presents the validation of the single-perturbation, non-linear regression method of measuring human arm stiffness for the purpose of future overground pHRI applications. Since no prior art reported arm stiffness measurements during overground pHRI, we compared our method with prior art with seated pHRI [8,9]. First, the method was used to estimate the stiffness of passive mechanical springs with known stiffness values. Then, human experiments with tasks similar to [8] and [9] were conducted to compare the arm stiffness values obtained with different methods. The interpretation of the overall results and their implications are also presented.

## 2. METHODS

Our stiffness estimation method is extensively described in [5, 11], but is briefly summarized here. During an overground pHRI experiment, a human user holds the handle of the robot arm while walking together with Ophrie. The robotic arm

provides small restoring forces to keep the hand near the center of the workspace of the robot arm throughout the experiment, except during the force perturbation. The interaction forces and the hand position (= handle position) are recorded. For short durations, the arm dynamics can be expressed in a 2nd order linear equation:

$$f-f_0=m(\ddot{x}-\ddot{x}_0)+b(\dot{x}-\dot{x}_0)+k(x-x_0) \quad (1)$$

where  $m$ ,  $b$ , and  $k$  are the arm inertia, damping, and stiffness, respectively, and  $f$  is the interaction force, and  $x$  is the position of the handle.

The subscript  $\cdot_0$  implies the measurement values at the onset of the perturbation at  $t = 0$ . The data during the time interval  $[0, T]$  is used to estimate  $m$ ,  $b$ , and  $k$  with multi-variable linear regression in Matlab, where  $T$  is determined by the timing of the first maximum (second extremum) of the velocity profile, as discussed in [5, 11], which is typically 300 ~ 500 ms in this task.

A notable feature of this stiffness estimation method, as compared to well-known methods used in [8] or [9], is that this method only requires a short period of time. This makes this technique suitable for overground pHRI experiments.

The experiment presented in this work involved the Ophrie robot [5, 11], shown in Figs. 1 and 2. Briefly, the robot has an interaction handle with a force sensor to acquire the 6-axis interaction forces, where the force in the perturbation direction is used for (1). The interaction handle sits at the junction of two distal handles of the 5-bar linkage. The mechanism is driven by two servo motors, each equipped with its own encoder, and are attached on either side of the ground link.

## 2.1. PASSIVE SPRING EXPERIMENT

To validate the above stiffness estimation technique on a passive mechanical setup with known stiffness, we first applied this method on a customized spring setup (Fig. 2).

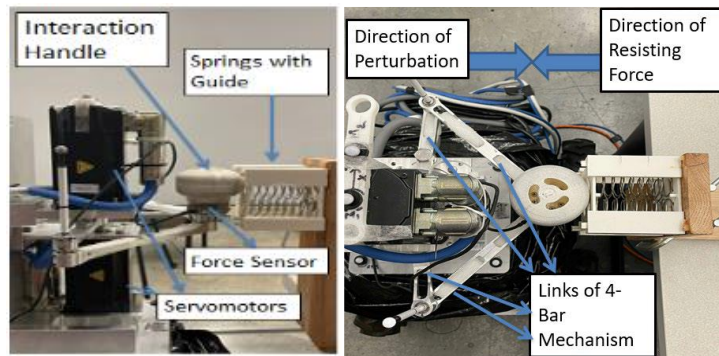


Figure 1. Passive spring setup: front view (Left) and top view (Right).

The setup consisted of 2, 3, or 4 springs in parallel, where each spring (Lee's Springs, TN, USA) had a stiffness of 96.494 N/m with  $\pm 10\%$  error range according to the manufacturer. Hence, this setup provided roughly 200-400 N/m of stiffness, comparable to typical values of arm stiffness in the literature [8-10]. Due to the moving parts of this setup, substantial damping and/or friction was present which was reduced by polishing and lubrication.

The interaction handle was positioned such that it is near the center of the workspace of the robot arm. Then, the spring setup was positioned such that the robot handle was in contact with the plate to which all springs were attached as shown in Fig. 1. Perturbation was applied to the interaction handle and the forces commanded onto

the interaction handle along with the displacement of the springs were recorded. For each setup (2, 3, or 4 springs), 10 trials were conducted.

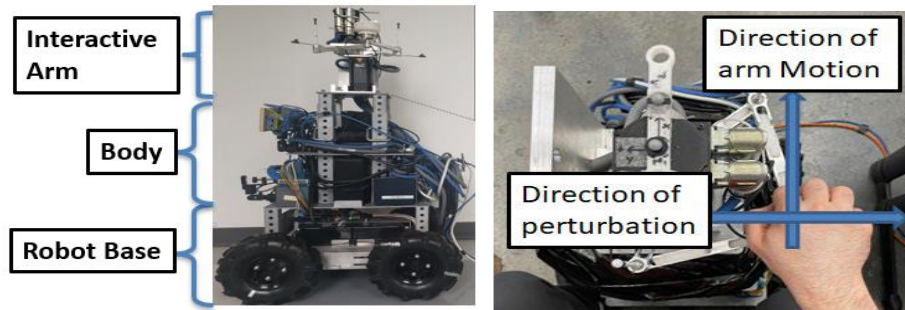


Figure 2. Photo of Ophrie (Left) and the human experiment set up (Right). In static trials the hand is positioned in the center of the workspace of the robot arm. In dynamic trials, the hand moves in forward direction as shown in the right figure.

A separate verification experiment was performed to identify the effect of friction in the CCF condition. As constant force was commanded, the end effector was pushed manually by the hand of the experimenter. The interaction force and the position information of the end effector from the haptic device were obtained and compared.

## 2.2. SEATED HUMAN EXPERIMENT

To validate the above stiffness estimation technique on a passive mechanical setup with known stiffness, we first applied this method on a customized spring setup (Fig. 2).

While the presented stiffness estimation method was developed for overground pHRI experiments, for accurate comparisons with prior work, the human experiments

presented in this work were in seated positions [8, 9]. Also, the tasks in this experiment were intended to be similar to those in [8] and [9], such that the results from our stiffness estimation method could be deliberately compared with results from the prior art.

Nine healthy young adults with no self-reported history of neurological disorders were recruited for this study ( $23.9 \pm 5.6$  years of age, 5 females). The experimental protocols and procedures were approved by the Institutional review board (IRB) of the University of Missouri. All the subjects have given their written, informed consent.

Subjects were seated in front of the robot with their hand placed on the interaction handle positioned directly in front of them. This was to acquire the arm stiffness in poses that are similar to those in [8] or [9]. The subjects were instructed to keep their eyes closed during the entire period of the trial. They were also instructed to focus on their tasks while there may be gentle pushes from the robot. The arm stiffness was measured for two conditions: static and dynamic. In the static condition, the perturbations were provided by the robot when they maintained their hand near the center of the workspace of the robot arm as shown in Fig. 2. For the dynamic condition, the robot would provide perturbations to the human hand while they moved their hand in the forward direction as shown in Fig. 2. The duration of the movement was approximately 1 second, and the length of the movement path was approximately 10 cm.

For each subject, the experiment included 10 blocks of 11 trials each (10 dynamic and 1 static trials), with a total of 110 trials. Half of the dynamic trials (5 per

block, randomized in order) did not provide perturbation. This was to ensure that the subjects would not know which trial had a perturbation and therefore to not modify their behavior in anticipation to perturbation. For analysis, only the dynamic trials with perturbations were used. After the completion of each set of the 10 dynamic trials, one static trial was conducted to conclude the block. Since the static and dynamic trials had different protocols, their order was not randomized.

### **2.3. DATA ANALYSIS**

To analyze the data from the passive spring setup, the stiffness from each trial was calculated using Eq. (1) as described earlier. Using the data from 2, 3, and 4 spring configurations, a linear fit with the stiffness as a function of the number of springs was obtained.

For the human experiments, data from 50 dynamic trials and 10 static trials were used for each subject. arm stiffness was estimated using Eq. (1) as described earlier. When appropriate, *t*-tests were applied to investigate notable differences in experimental conditions. The normality of the data was verified before the application of *t*-tests.

## **3. RESULTS**

### **3.1. RESULTS FROM THE PASSIVE SPRING EXPERIMENTS**

Fig. 3 shows the estimated stiffness of the spring setup consisting of 2, 3, and 4 springs in parallel. The estimated stiffness values of each setup were

192.630±19.263N/m, 288.900± 28.890N/m, and 385.27± 38.527N/m for 2, 3, and 4 springs, respectively. The time interval of data used for the analysis was  $T = 115.935±8.421$  ms. The linear regression showed a slope of 96.908 N/m with an intercept of 7.071 N/m ( $R^2 = 0.8823$ ). The estimated spring stiffness is within 0.5% of the manufacturer-provided stiffness.

### 3.2. RESULTS FROM SEATED HUMAN EXPERIMENTS

Out of a total of 450 dynamic trials (9 subjects, 50 trials with perturbation each) and 90 static trials (9 subjects, 10 trials each), data from 8 trials were identified as obvious outliers (negative value of stiffness) and were discarded from the analysis. These negative stiffness values may come from human movement artifact and/or regression method. Nonetheless, over 98.5% of data were considered. The time interval of data used for this analysis was  $T = 323.096±54.352$  ms. Shapiro-Wilk test for normality showed that the overall data was not non-normal ( $p<0.001$ ). In addition, both datasets for static and dynamic conditions were also not non-normal (both  $p<0.001$ ). This allowed applying the  $t$ -tests. The size of the standard deviation of data with respect to the mean was comparable to similar works involving human subjects [5,11].

The estimated arm stiffness for each subject is shown in Fig. 4. As expected, the arm stiffness varied across the subjects. Altogether, the arm stiffness in the static pose was  $100.092±56.440$  N/m, whereas, in dynamic condition, it was  $68.470±35.278$  N/m. The arm stiffness values were significantly different between the static and dynamic conditions (Fig. 5A,  $p<0.001$ ). In the static condition, the learning effect of the subjects was found to be significant (Fig. 5B,  $p<0.02$ ). The static arm stiffness in

the first 5 blocks was  $115.518 \pm 7.050$  N/m, while in the last 5 blocks, the stiffness was  $85.694 \pm 7.516$  N/m. On the other hand, the arm stiffness in the dynamic condition did not show significant differences between the first 5 and the last 5 blocks ( $67.1582 \pm 43.741$  N/m and  $69.899 \pm 35.976$  N/m, respectively).

The stiffness values for static and dynamic conditions were compared with those in existing literature [8, 9] as shown in Fig. 6. Considering the means of each subject, the arm stiffness in the static pose in this work was similar to the values reported in [8, 9]. In contrast, when the arm was moving, [8] reported the arm stiffness of  $106.050 \pm 15.963$  N/m, while in dynamic conditions of our experiment, the arm stiffness was  $68.592 \pm 11.031$  N/m.

#### 4. DISCUSSION

The validation of our stiffness estimation technique with a passive spring setup highlighted the accuracy of the method. Despite non-negligible, non-linear, and non-repeatable friction and damping in the setup, with 10 trials on each stiffness value, our method was able to correctly estimate the stiffness value within 0.5% of the rated stiffness with a high  $R^2$ . The variance between trials is likely from static friction since the amount of variance does not seem to scale with the number of springs used in the setup.

It should be noted again that the proposed stiffness estimation method was developed for overground pHRI experiments, in which opportunities to apply

perturbations (which are necessary for arm stiffness estimation) are short and far between.

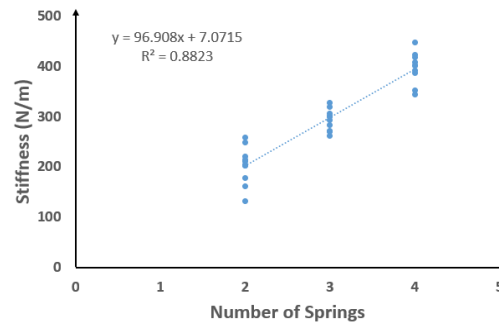


Figure 3. Linear regression of stiffness measurement from spring experiments using 2, 3, and 4-spring configurations.

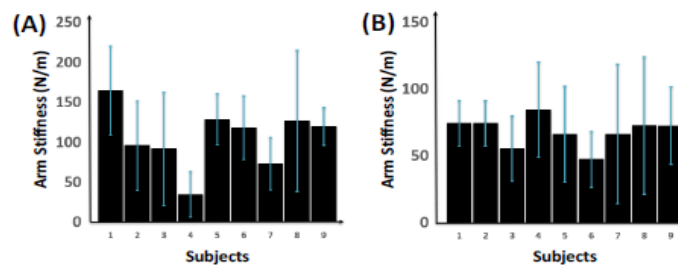


Figure 4. Arm stiffness estimated for each subject. (A) static condition, (B) dynamic condition.

In this case, most stiffness methods proposed in [8-10] cannot be applied. However, in order to validate this method, experimental settings were used that are similar to well-accepted prior work of [8] and [9], which did not involve overground pHRI. On these grounds, the result from our method is comparable with the prior works.

Since the perturbation was only in the lateral direction in our experiment, only the respective component of the arm stiffness reported in [8] and [9] was extracted to be compared with our work. For the static condition, the task in our experiment is very similar to those in [8] and [9] since the arm poses were similar and factors regarding

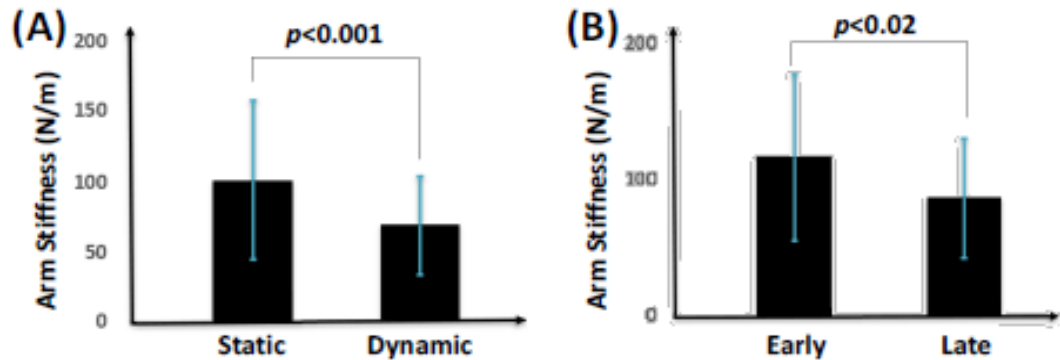


Figure 5. Sensitivity of arm stiffness estimation method to reveal the differences between (A) experimental conditions, and (B) learning effect between early and late trials within static trials.

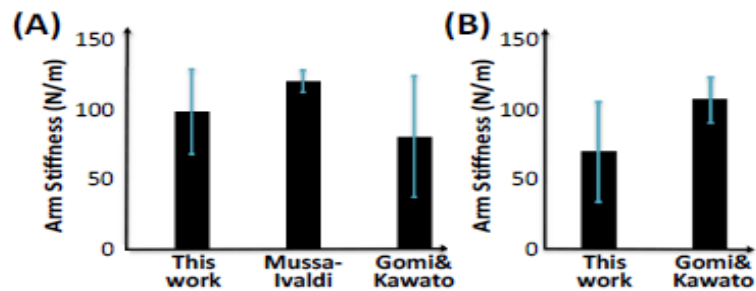


Figure 6. Arm stiffness comparison between this work, Gomi& Kawato [8], and Mussa-Ivaldi et al. [9]. (A) static condition (B) dynamic condition.

the differences in the apparatus, such as the mechanical impedance or the size of the workspace, did not affect the experiment. However, fine details may have been different, such as the specific instructions to the subjects or the shape and feel of the

handle. Nonetheless, the arm stiffness in the static condition was very similar to those reported in [8] and [9], highlighting the validity of the stiffness estimation method used in this work.

On the other hand, the arm stiffness in dynamic trials showed notable differences between this work and [8]. The arm stiffness in the dynamic condition in our experiment was lower than the arm stiffness during forward reaching movement in [8]. This may be due to several key differences in the experimental task that may affect the modulation of arm stiffness in humans. For example, in our experiment, the subjects' eyes were closed, and the distance of forward arm movement was much less than in [8] (10 cm versus 40 cm). The small workspace of the arm of Ophrie may have challenged the subjects to generate more accurate movement to stay within the workspace. These factors may have compelled the subjects to become more sensitive about the ongoing interaction task, which in turn may have decreased the arm stiffness [13, 14]. Despite these differences, the arm stiffnesses in this work and [8] were comparable in magnitude, further validating the stiffness estimation method used in this work. It is also interesting to note that our method was able to differentiate static versus dynamic conditions (Fig. 5A) whereas in [8], the stiffness values were similar between these conditions.

While learning effects are common in human experiments (for example, in [3]), they were observed in the static condition but not in the dynamic condition. This may be because there were 10 times more dynamic trials than static trials, such that learning may have occurred and settled in the first 1 or 2 blocks of dynamic trials. Although the scope of this work does not include the investigation of the learning effects, it should

be noted that the stiffness estimation method used in this study is sensitive enough to capture possible learning effects as shown in Fig. 5B.

## 5. CONCLUSION

This work presented the validation of an arm stiffness estimation method using force perturbations and multivariable linear regression. The method successfully estimated the stiffness of passive springs with known stiffness values. In addition, human arm stiffness values estimated with this method were comparable with those in the prior art. The characteristics of this method, such as requiring only short perturbations, are ideal for estimating human arm stiffness during overground pHRI interaction experiments. As such, we expect this method to be widely useful for understanding the biomechanics of physical interactions in practical overground pHRI scenarios, such as when a robot guides a human follower to walk.

## REFERENCES

- R. Alami et al., "Safe and dependable physical human-robot interaction in anthropic domains: State of the art and challenges," *2006 IEEE/RSJ International Conference on Intelligent Robots and Systems*, Beijing, China, 2006, pp. 1-16.
- S. Haddadin, A. Albu-Schäffer, G. Hirzinger, "Safe Physical Human-Robot Interaction: Measurements, Analysis and New Insights". In: Kaneko, M., Nakamura, Y. (eds) *Robotics Research. Springer Tracts in Advanced Robotics*, vol 66, 2010.
- F. Sylos-Labini, A. d'Avella, F. Lacquaniti, and Y. Ivanenko, "Human-human interaction forces and interlimb coordination during side-by-side walking with hand contact". *Frontiers in physiology*, 9, March, 2018, p. 179.E

- A. Q. Keemink, H. van der Kooij, and A. H. Stienen, "Admittance control for physical human-robot interaction." *The International Journal of Robotics Research*. 2018;37(11), pp. 1421-1444
- S. Regmi, D. Burns, and Y. S. Song, "Humans modulate arm stiffness to facilitate motor communication during overground physical human-robot interaction," *Scientific Reports*, 12(1), 2022.
- G. L. Holmes, K. M. Bonnett, A. Costa, D. Burns and Y. S. Song, "Guiding a Human Follower with Interaction Forces: Implications on Physical Human-Robot Interaction," *2022 9th IEEE RAS/EMBS International Conference for Biomedical Robotics and Biomechatronics (BioRob)*, Seoul, Korea, 2022, pp. 1-6.
- M. Wu, L. Drnach, S. M. Bong, Y. S. Song, and L. H. Ting, "Human-Human Hand Interactions Aid Balance During Walking by Haptic Communication," *Frontiers in Robotics and AI*, 2021.
- H. Gomi and M. Kawato, "Human arm stiffness and equilibrium-point trajectory during multi-joint movement." *Biol Cybern.* 1997 Mar;76(3), pp.163-71.
- T. Flash and F. A. Mussa-Ivaldi, "Human arm stiffness characteristics during the maintenance of posture," *Experimental Brain Research*, 82(2), 1990, pp. 315–326.
- R. D. Trumbower, M. A. Krutky, B. S. Yang, and E. J. Perreault, "Use of self-selected postures to regulate multi-joint stiffness during unconstrained tasks," *PLoS ONE*, 2009;4(5):e5411.
- S. Regmi, D. Burns, and Y. S. Song, "A robot for overground physical human-robot interaction experiments," *PLoS ONE* 17(11), 2022.
- S. Regmi and Y. S. Song, "Design Methodology for Robotic Manipulator for Overground Physical Interaction Tasks". *Journal of Mechanism and Robotics*, 12(4), August, 2020, p. 041002.
- F. Rashid, D. Burns, and Y. S. Song, "Factors affecting the sensitivity to small interaction forces in humans," *2021 43rd Annual International Conference of the IEEE Engineering in Medicine & Biology Society (EMBC)*, 2021, pp. 6066-6069.
- F. Rashid, D. Burns, and Y. S. Song, "Sensing small interaction forces through proprioception," *Scientific Reports*, 11(1), 2021, pp. 1-10.

## SECTION

### 2. FURTHER DISCUSSION AND DATA ANALYSIS

#### 2.1. DATA EXTRACTION FROM PRIOR ART

The motivation for this work was to develop an overground robot that can physically interact with human beings, and we have chosen arm stiffness measurement as our prime objective of interest. Thus, for this purpose we have heavily relied on the arm stiffness estimation technique mentioned in [10] and the arm stiffness modulation characteristics described in [11] to develop an Overground robot that can measure Arm stiffness. Also [10] was the only work existing in literature that exclusively developed an arm stiffness measurement method in static condition. And [11] was the only work that reported arm stiffness values in both static and dynamic conditions. So, we developed our measurement technique that draws parallels to the methods used in [10] and [11]. This was done to ensure that meaningful comparisons can be made between our method and that of theirs.

However, there are some challenges in directly adopting their techniques to build our robot. Some of the challenges like number of trials, duration of trials have been discussed in the previous section of this work. Apart from them the key challenge was obtaining the numerical values of arm stiffness reported in their work. Their work(s) have only graphical representation of the arm stiffness and they have not mentioned those values anywhere in their work. To infer from these figures, we had to rely on data interpretation method for estimating the numerical values of their reported

stiffness values. As depicted in Figure 2.1, the ellipses are a representation of arm stiffness of the subjects are shown as ellipses. The major axis of ellipse represents the direction in which the arm stiffness is high for the subject and the minor axis represents the direction in which arm stiffness is low for that particular subject.

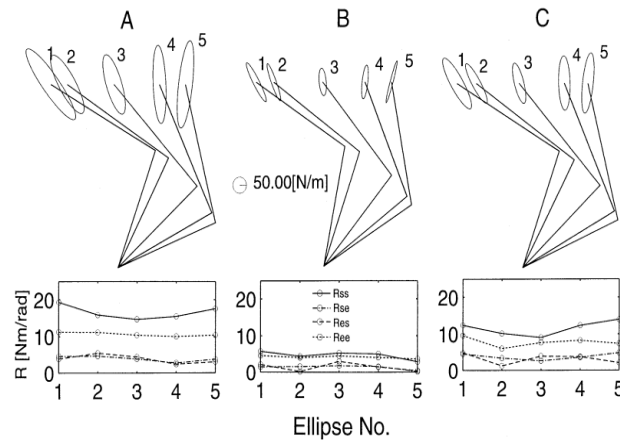


**Fig. 2.** Stiffness ellipses (*upper figures*) and joint stiffness values (*lower figures*) during posture maintenance of subjects *A*, *B*, and *C*. During the experiments, the subjects were asked to relax and not to exert any force against PFM, assisted by visual feedback of a force vector on the computer monitor (see Fig. 1 and Static-stiffness experimental procedure in the text). The visual feedback was frozen during perturbation

Figure 2.1. Arm stiffness ellipses reported in [10] for static condition.

So, we used the pixel resolution method to infer the arm stiffness values from their work. Since these ellipses were drawn to scale with the representation of 50N/m, we used the pixel method in paint software to calculate the arm stiffnesses of each subject. Our method of stiffness measurement uses perturbation in the X-X direction for the static condition, and the movement of hand in the positive Y-Y direction for dynamic trials. However as depicted in Figure 2.1 the subjects of [8] displayed arm stiffnesses in directions that are at an angle to the X-Y coordinate system. Thus, we used the component of their stiffnesses in the X-X direction. [10] has 3 subjects in their

study. The ellipses#3 in Figure 2.1 represents the posture maintenance that is very similar to the static trial protocol of our study.

As depicted in Figure 2.2, the 50 N/m represented in the circle is analyzed in paint software to determine the distance between the center and the end of the circle. This gives an estimate of how many pixels in the horizontal direction represent this 50 N/m.

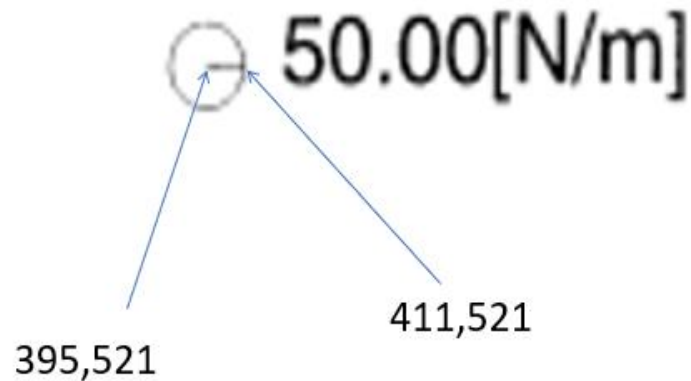


Figure 2.2. Pixel representation of the 50N/m reference used in [10] to compute the stiffnesses of the 3 subjects used in their study.

The center line is represented by the pixels 395,521 and 411,521. Thus 16 pixels represent 50 N/m. Using this estimate the horizontal stiffnesses of three subjects in [10] are calculated. The pixel value of their stiffnesses in X-X direction are depicted in Figure 2.3. Using the method of extrapolation, the difference in the pixel values of the stiffnesses is calculated and multiplied the representation factor to obtain the stiffness of all the three subjects mentioned in [10].

For subject A, the difference in the pixel representation is  $196-175=21$ . His/her stiffness is given by:

$$\frac{21}{15} * 50 = 65.$$

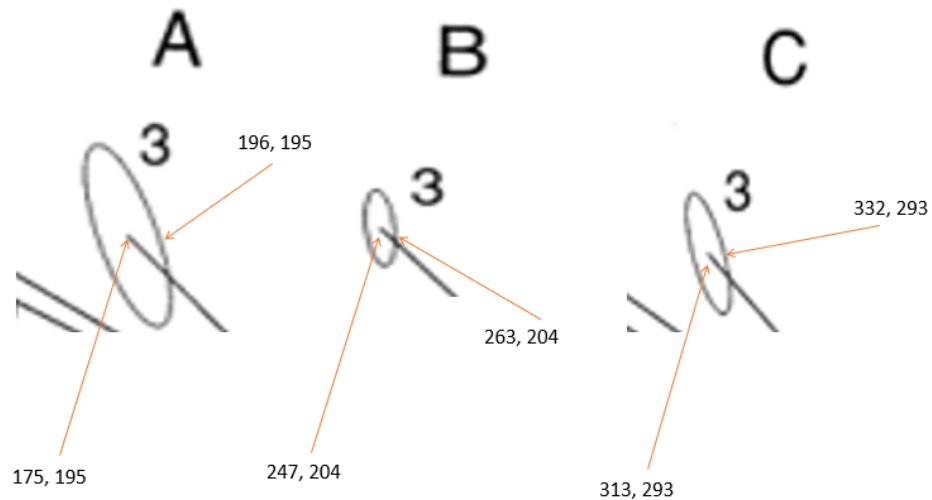


Figure 2.3. Pixel representation of the stiffnesses of the 3 subjects used in the study of [10].

Hence the full stiffness for subject A is twice this calculation, which turns out to be 130. Similarly using the pixels values mentioned in Figure 2.3, the arm stiffnesses values of subjects B, and C are calculated and found to be 50 N/m and 60 N/m.

Using the same pixel method the dynamic stiffness values of the subjects reported in [10] are computed for comparing the stiffness values of the subjects in our study.

## 2.2. DATA ANALYSIS FOR LEARNING EFFECT

As discussed in Chapter 1 of this work, the trials for the subjects were conducted in static and dynamic condition. For every subject 100 trials (50 with perturbation and 50 without perturbation) in dynamic condition and 10 static condition were given to obtain the arm stiffness data of those subjects. The purpose of these large number of trials was to check if there is any learning effect in the subjects over the trials. The 110 trials were divided into 10 blocks with each block containing 11 trials (5 trials in dynamic condition with perturbation+ 5 trials in dynamic condition+ 1 trial in static condition). It must be mentioned that the 10 trials in dynamic condition were completely randomized. After these 10 trials the static trial was conducted.

For the analysis of these 10 blocks, the first 3 blocks were called early trials, the next 4 blocks were classified as middle trials, and the last 3 blocks were classified as late trials.

**2.2.1 Early Versus Late Trials.** The Analysis of Variance (ANOVA) and the effects test between the first 3 trials and last 3 trials are depicted in Table 2.1. The P-value for ANOVA and 3-way interaction is 0.0001. This means that the arm stiffness is significantly different between the first 3 and the last 3 trials. Also, it indicates that the subject, arm condition, and learning effect are significantly affecting the Arm stiffness.

**2.2.2 Early Versus Middle Trials.** The Analysis of Variance (ANOVA) and the effects test between the first 3 blocks and next 4 blocks are depicted in Table 2.2. The P-value for ANOVA and 3-way interaction is 0.0002. This means that the arm stiffness is significantly different between the first 3 and the next 4 blocks. Also, it

indicates that the subject, arm condition, and learning effect are significantly affecting the Arm stiffness.

Table 2.1. ANOVA and Effects Summary for Early Versus Late Trials

<b>Analysis of Variance (ANOVA)</b>					
Source	Degrees of Freedom	Sum of Squares	Means Square	F-Ratio	Significance
Model	35	267489.28	7642.55	5.948	0.0001*
Error	497	638597.08	1284.9		
Total	532	906086.37			
<b>Effects Test</b>					
Source	Number of Parameters	Degrees of Freedom	Sum of Squares	F-Ratio	Significance
Subject	8	8	40840.265	3.97	0.0001*
Arm Condition	1	1	60594.78	47.15	0.0001*
Learning Effect	8	8	69729.82	6.78	0.0001*
Subject* Arm Condition	1	1	12697.74	9.88	0.0018*
Learning Effect* Arm Condition	8	8	52554	5.11	0.0001*
Subject* Learning Effect	1	1	18289.15	14.23	0.0002*
Subject* Learning Effect* Arm Condition	8	8	25526	2.48	0.012*

\* Indicates it is significant

**2.2.3 Static Trials.** The static data of all the subjects were grouped into two blocks (Early and Late) and analyzed. The ANOVA results are presented in Table 2.3. It can be inferred that the model is significant and the 2-way interaction between subject and learning effect is also significant. The subjects had lower stiffness during the late trials. The average stiffness during the first 5 blocks was 113.58 N/m while that in the last

5 blocks was 83.18 N/m. It must be mentioned here that the arm stiffness is significantly different for all the subjects in Early and late trials.

Table 2.2. ANOVA and Effects Summary for Early Versus Middle Trials

<b>Analysis of Variance (ANOVA)</b>					
Source	Degrees of Freedom	Sum of Squares	Means Square	F-Ratio	Significance
Model	37	262343.4	7090.36	6.3536	0.0001*
Error	336	374964.84	1115.97		
Total	373	906086.37			
<b>Effects Test</b>					
Source	Number of Parameters	Degrees of Freedom	Sum of Squares	F-Ratio	Significance
Subject* Arm Condition	2	1	14909.99	12.64	0.0004*
Learning Effect* Arm Condition	16	8	59982.6	6.71	0.0001*
Subject* Learning Effect	2	1	7410.02	6.64	0.0104*
Subject* Learning Effect* Arm Condition	16	8	34843.95	3.90	0.0002*

\* Indicates it is significant

**2.2.4 Dynamic Trials.** The Dynamic data of all the subjects were grouped into two blocks (Early and Late) and analyzed. The ANOVA results are presented in Table 2.4. It can be inferred that the model is significant and only the subject was significant.

From these four distinct analyses it can be inferred that the 3-way interaction was found to be significant in Early-middle blocks and Early- Late blocks. It means that the arm stiffness is significantly different for Early, Middle, and Late blocks in both static and dynamic conditions. Thus, we choose to group the first 5 blocks as

Early and last 5 blocks as late trials to perform the analysis, which has been discussed in chapter.1 of this work.

Table 2.3. ANOVA and Effects Summary for Static trials

<b>Analysis of Variance (ANOVA)</b>					
Source	Degrees of Freedom	Sum of Squares	Means Square	F-Ratio	Significance
Model	17	122568.85	7209.93	3.3081	0.0002*
Error	68	148202.98	1279.46		
Total	85	270771.83			
<b>Effects Test</b>					
Source	Number of Parameters	Degrees of Freedom	Sum of Squares	F-Ratio	Significance
Subject	8	1	51637.05	2.96	0.0067*
Learning Effect	1	1	18950.36	8.69	0.0044*
Subject* Learning Effect	8	8	42315.71	2.42	0.0227*

\* Indicates it is significant

Table 2.4. ANOVA and Effects Summary for Dynamic trials

<b>Analysis of Variance (ANOVA)</b>					
Source	Degrees of Freedom	Sum of Squares	Means Square	F-Ratio	Significance
Model	17	64096.16	3770.36	3.2972	0.001*
Error	248	489425.67	1143.52		
Total	445	553521.83			
<b>Effects Test</b>					
Source	Number of Parameters	Degrees of Freedom	Sum of Squares	F-Ratio	Significance
Subject	8	1	48512.37	5.5	0.0001*
Learning Effect	1	1	809.63	0.7	0.4006
Subject* Learning Effect	8	8	15110.89	1.65	0.1083

\* Indicates it is significant

### 3. FORCE-VELOCITY AND FORCE-ACCELERATION ANALYSIS

To demonstrate a practical application of pHRI using Ophrie, we proposed an experimental condition consisting of dyads. This was motivated by the work of [17], which uses the concept of executor and conductor in a physical interaction based on the signals of the force, velocity, and acceleration. This section discusses the proposed methodology by [17] along with their mathematical model for determining these roles in a dyadic physical interaction. Further we have empirically applied their model to our robot in three distinct cases: the Ophrie handle acting as background stiffness, as a damper, and as an inertial mass.

To determine the role played by each member of the dyad, [17] has proposed two terms: executor and Conductor. Broadly the term conductor refers to the person who takes the decision and controls the motion, while executor refers to the person who accomplishes the motion. However, these two roles are not exclusive. At any given time, a member of the dyad can play the role of both executor and conductor.

#### 3.1. FORCE, VELOCITY, ACCELERATION CONVENTION

Consider two forces applied at a point. According to Newton's third law applied force and reactive force have the same absolute value and reverse signs. These forces can be considered as forces applied by each partner at the point of interaction. Let  $f_i$  be the net interaction force due to the forces applied by the partners at the point of interaction. For the purposes of analysis this  $f_i$  is considered positive if the point of interaction is squeezed, and it is considered negative if the point of interaction is

stretched. Also, the displacement, velocity, and acceleration are considered positive when they are happening in the positive direction of X-axis. And they are considered negative if they are in the negative direction of X-axis. This nomenclature is depicted in Figure 3.1

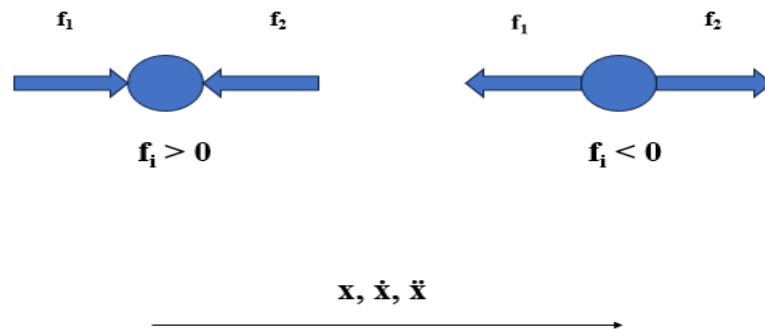


Figure 3.1. Force, Displacement, Velocity and Acceleration depiction in a dyad interaction.

Note that the measured interaction force does not affect the motion directly. Motion in positive and negative direction can happen for both positive and negative interaction force. In other words, just looking at their sign of  $f_i$  one cannot determine the direction of motion.

### 3.2. EXECUTORSHIP: FORCE-VELOCITY RELATION

Consider the interaction is moving with positive velocity (to the right) and the measured force is positive. It means the partners are pushing against each other and the left partner is applying more force, while the right partner is applying a reactive force. Hence the left partner is the executor because the direction of applied force coincides

with the direction of velocity. Imagine now if the right partner applies more force so that direction of velocity changes and becomes negative. Hence for a positive interaction force and negative velocity the right partner becomes the executor. So, for a positive interaction force, the sign of velocity reveals the executor of the task. Hence, we can conclude that looking at the signs of velocity and interaction we can determine which partner is a executor. If  $\lambda$  denotes the executor in a task, it can be determined by the expression:

$$\lambda = - \text{Sign}(f_i) \text{Sign}(\dot{x}) \quad (3.1)$$

### 3.3. CONDUCTORSHIP: FORCE-ACCELERATION RELATION

To determine which partner initiates changes in motion, dynamics of motion must be investigated, Consider two scenarios where change in individual forces  $f_1, f_2$  do not cause change in interaction force,  $f_i$ . First, the executor increases the force she/he applies and consequently the velocity increases. Second, the partner increases his/her force and velocity decreases. This can be interpreted as the decision of follower to change the direction of motion, which leads to change in the direction of velocity. Also increased magnitude of interaction force doesn't change the velocity sign immediately. Hence, we must consider a phase of deceleration provoked by applied force of passive partner.

It can be stated that for a positive interaction force, if the acceleration is negative the follower applies a force that slows down the system. This tells that the follower is the conductor. Analogously, if  $f_i$  changes its sign and becomes positive, it means that the executor decides to change the direction of motion, and he/she becomes

conductor as he/she increases the force. Thus, the expression for conductorship can be given by:

$$\chi = - \text{Sign}(f_i) \text{Sign}(\ddot{x}) \quad (3.2)$$

### 3.4. OPHRIE AS A CONDUCTOR-EXECUTOR

Most Physical Human Robot Interaction (pHRI) models are derived from concepts and experiments in Physical Human Interaction (pHHI) Experiments. The concept of executor and conductor discussed in [17] is applied to the Ophrie handle interacting with human subject to determine the roles of conductor and executor based on the expressions 3.1 and 3.2. The Ophrie handle is assumed to be moving to-and-from from the mean position. The schematic is depicted in Figure 3.2.

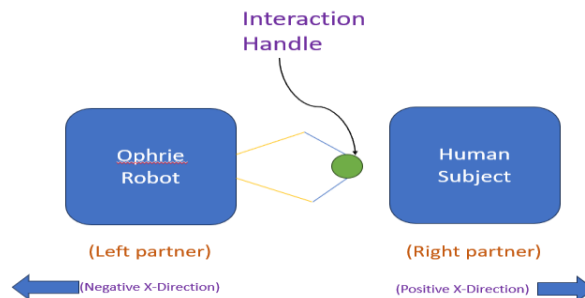


Figure 3.2. Schematic of the Human Ophrie set-up for executor conductor role determination in different conditions.

**3.4.1 Ophrie Handle Acting As A Background Stiffness.** If the Ophrie handle is acting as a stiffness, then the force it exerts is directly proportional to the displacement, given by the expression:

$$F = k \cdot x \quad (3.3)$$

Where  $k$  is the stiffness of the handle in N/m and  $x$  is the displacement of the handle.

As depicted in Figure 3.2, the force profile is identical to the Displacement profile. The roles of executor and conductor played by the human subject and the robot are calculated by the expressions (3.1) and (3.2) and depicted in Table(s) 3.1 and 3.2.

The change of roles are depicted in Figure 3.2.

Table 3.1: Executorship determination in background stiffness

Displacement Direction	Velocity	Force	$-\text{Sign}(f_i) \cdot \text{Sign}(\dot{x})$	Executor
$X > 0$	$\dot{x} > 0$	$f_i < 0$	+1	Human (Right Partner)
$X > 0$	$\dot{x} < 0$	$f_i < 0$	-1	Robot (left Partner)
$X < 0$	$\dot{x} < 0$	$f_i > 0$	+1	Human (Right partner)
$X < 0$	$\dot{x} > 0$	$f_i > 0$	-1	Robot (left Partner)

Table 3.2: Conductorship determination in background stiffness

Displacement Direction	Acceleration	Force	$-\text{Sign}(f_i) \cdot \text{Sign}(\ddot{x})$	Conductor
$X > 0$	$\ddot{x} > 0$	$f_i < 0$	+1	Robot (left partner)
$X > 0$	$\ddot{x} < 0$	$f_i < 0$	-1	Robot (left partner)
$X < 0$	$\ddot{x} < 0$	$f_i > 0$	+1	Human (Right Partner)
$X < 0$	$\ddot{x} > 0$	$f_i > 0$	-1	Robot (left partner)

**3.4.2 Ophrie Handle Acting As A Damper.** If the Ophrie handle is acting as a Damper, then the force it exerts is directly proportional to the velocity, given by the expression:

$$F = B \cdot \dot{x} \quad (3.4)$$

Where  $B$  is the Damping coefficient of the handle and  $\dot{x}$  is the velocity of the handle.

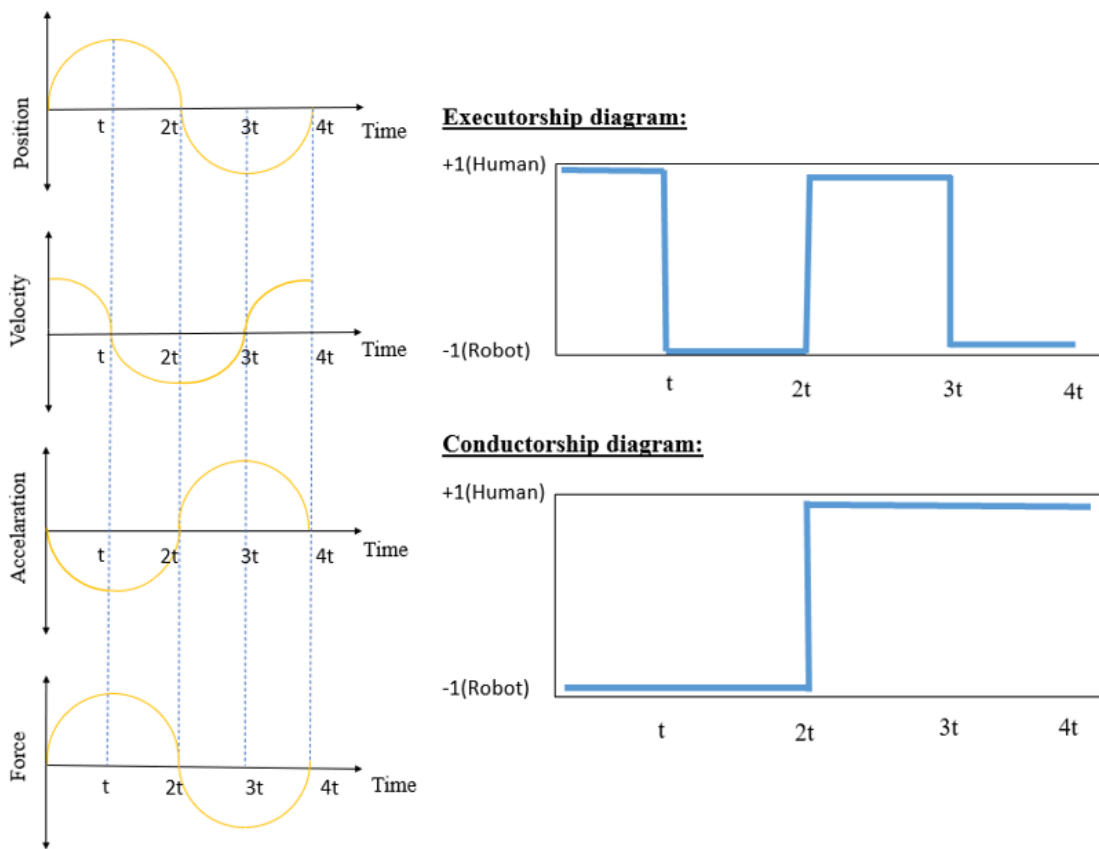


Figure 3.3. The variation of force, displacement, velocity, and acceleration on Ophrie handle acting as a background stiffness. (Right) The executor and conductor Roles exhibited by Human subject and Ophrie handle during background stiffness condition.

As depicted in Figure 3.2, the force profile is identical to the Velocity profile. The roles of executor and conductor played by the human subject and the robot are calculated by the expressions (3.1) and (3.2) and depicted in Table 3.3. The change of roles are depicted in Figure 3.3.

Table 3.3: Executorship determination in Damping Condition.

Displacement Direction	Velocity	Force	$-\text{Sign}(f_i) \cdot \text{Sign}(\dot{x})$	Executor
$X > 0$	$\dot{x} > 0$	$f_i < 0$	+1	Human (Right Partner)
$X > 0$	$\dot{x} < 0$	$f_i < 0$	+1	Human (Right Partner)
$X < 0$	$\dot{x} < 0$	$f_i > 0$	+1	Human (Right partner)
$X < 0$	$\dot{x} > 0$	$f_i > 0$	+1	Human (Right Partner)

Table 3.4: Conductorship determination in Damping condition.

Displacement Direction	Acceleration	Force	$-\text{Sign}(f_i) \cdot \text{Sign}(\ddot{x})$	Conductor
$X > 0$	$\ddot{x} > 0$	$f_i < 0$	+1	Robot (left partner)
$X > 0$	$\ddot{x} < 0$	$f_i < 0$	-1	Human (Right Partner)
$X < 0$	$\ddot{x} < 0$	$f_i > 0$	+1	Robot (left partner)
$X < 0$	$\ddot{x} > 0$	$f_i > 0$	-1	Human (Right Partner)

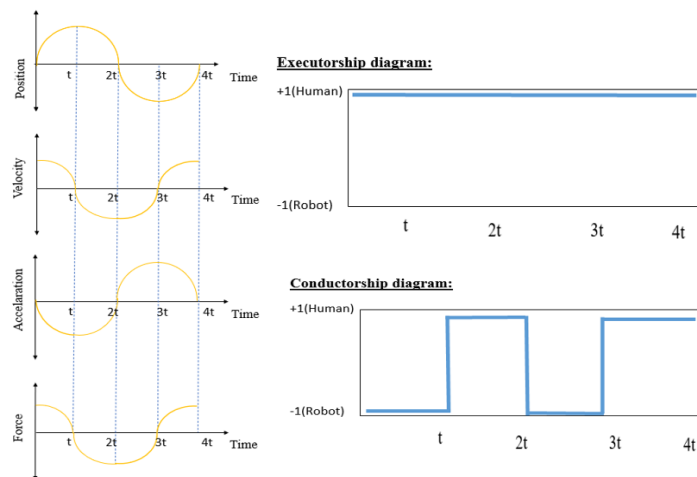


Figure 3.4. The variation of force, displacement, velocity, and acceleration on Ophrie handle acting as a Damper. (Right) The executor and conductor Roles exhibited by Human subject and Ophrie handle during damping condition.

**3.4.3 Ophrie handle acting as an Inertial Mass.** If the Ophrie handle is acting as a inertial mass, then the force it exerts is directly proportional to the Acceleration, given by the expression:

$$F = M \cdot \ddot{x} \quad (3.5)$$

Where M is the mass of the handle and  $\ddot{x}$  is the acceleration of the handle.

As depicted in Figure 3.5, the force profile is identical to the acceleration profile. The roles of executor and conductor played by the human subject and the robot are calculated by the expressions (3.1) and (3.2) and depicted in Table(s) 3.5 and 3.6.

The change of roles are depicted in Figure 3.5.

Table 3.5: Executorship determination in Inertial mass Condition.

Displacement Direction	Velocity	Force	- Sign( $f_i$ ) .Sign( $\dot{x}$ )	Executor
$X > 0$	$\dot{x} > 0$	$f_i < 0$	+1	Human (Right Partner)
$X > 0$	$\dot{x} < 0$	$f_i < 0$	-1	Robot (Left Partner)
$X < 0$	$\dot{x} < 0$	$f_i > 0$	+1	Human (Right partner)
$X < 0$	$\dot{x} > 0$	$f_i > 0$	-1	Robot (Left Partner)

Table 3.6: Conductorship determination in Inertial mass condition.

Displacement Direction	Acceleration	Force	- Sign( $f_i$ ) . Sign( $\ddot{x}$ )	Executor
$X > 0$	$\ddot{x} > 0$	$f_i < 0$	-1	Robot (left partner)
$X > 0$	$\ddot{x} < 0$	$f_i < 0$	-1	Robot (Left Partner)
$X < 0$	$\ddot{x} < 0$	$f_i > 0$	-1	Robot (left partner)
$X < 0$	$\ddot{x} > 0$	$f_i > 0$	-1	Robot (Left Partner)

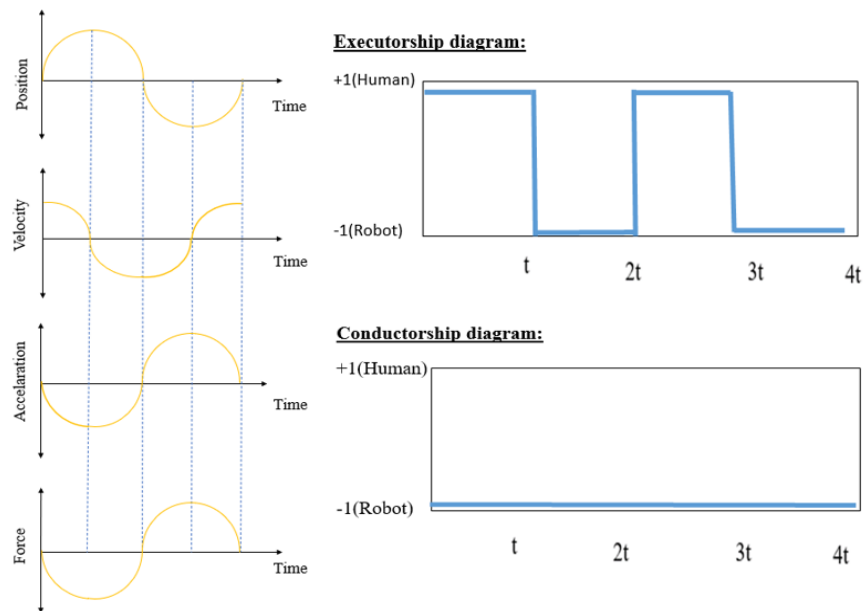


Figure 3.5. The variation of force, displacement, velocity, and acceleration on Ophrie handle acting as an Inertial mass. (Right) The executor and conductor Roles exhibited by Human subject and Ophrie handle during Inertial Mass condition.

### 3.5. DISCUSSION AND ANALYSIS

From the above three conditions the following inferences can be made:

- The human subject and Ophrie can exhibit the roles of both executor and Conductor simultaneously, as is evident in the Background stiffness condition. This tells us that being a background stiffness alone, the Ophrie can switch to either of the roles or actively play both the roles. The changes in the roles may have been due to the subject exhibiting a stiffness more or less than that of Ophrie's or may simply be due to the nature of the movement in this hypothetical experiment where humans act solely as a displacement source - which need further investigation.

- In the Damping condition, the executorship was solely exhibited by the Human subject while Ophrie was switching its role between conductorship and executorship. While these results are true per the sign convention method of [15], it cannot be explained by them alone.
- In the Inertial mass condition, the conductorship was solely exhibited by the Ophrie while the executorship was shared by both the Human subject and the Ophrie. While this may be true per the convention rules of [15], it cannot be logically deduced that an inertial mass can be a sole conductor.
- In all three cases, the robot acts only as passive elements (stiffness, damping, or inertia). That is, the robot cannot actively conduct or execute the interaction regardless of what the human partner does. However, applying the role assignment method in [15], the passive robot is still assigned conductorship or executorship, which also depends on the human movement. This implies that the method in [15], which is originally proposed for physical human-human interaction, cannot explain the role assignments during a certain subset of pHRI experiments where the robot is programmed to be passive (such as the case of OPHRIE).
- A more elaborate role assignment method may be required to study pHRI in each of these three cases. One possible way of quantifying the results will be to have subjects with known stiffness values participate in Interaction with Ophrie in all three scenarios. By setting the background stiffness of Ophrie to values above and below the corresponding stiffness values of the subject, we will be able to determine the dynamics of interaction.

## 4. CONCLUSIONS

This work has demonstrated a practical possibility of Physical Human Robot Interaction (pHRI). Our work used an Overground interactive robot that can measure arm stiffness. Since Humans can interact with robots with limbs as their first resort it is important to consider the characteristics of the human arm, which can be used to build overground robots. We have chosen Arm Stiffness as our subject of interest to pursue in that direction. Since there is very less literature in the field of arm stiffness measurement, we had to solely rely on them to compare our stiffness measurement method with that of theirs.

However, the key challenge in adopting their work directly was the number of trials, and the duration of perturbations. Our method uses a smaller number of trials compared to theirs, and in a short duration of perturbations. But the comparison of results between ours and theirs showed similarities. This validates our measurement technique. Moreover, the trials were conducted in a seated position to match the experimental conditions of theirs. The validated measurement in this work can be extended to new ideas like impedance matching, finding the arm stiffness characteristics differences between skilled personnel like physiotherapists and that of novices.

The force, velocity, and acceleration analysis discussed in Chapter 3 has been demonstrated empirically for our Ophrie interacting with a human subject. Though the results were based on the formulas discussed in the chapter, we can apply them experimentally using the arm stiffness method. This gives more insights on how future robots can be built to meet specific needs in healthcare and other applications.

**APPENDIX A.**  
**PARTICIPANT'S INFORMATION**

Table 1. Details of the Participants.

Subject	Subject Code	Gender	Age*
1	S01	F	22
2	S02	F	38
3	S03	F	24
4	S04	M	24
5	S05	F	18
6	S06	F	21
7	S07	M	24
8	S08	M	21
9	S09	M	23
10	S10	M	31

\*Age on the date of the experiment

**APPENDIX B.**

**SEQUENTIAL INSTRUCTIONS FOR THE EXPERIMENTER**

The consent form is given to the participant, and they are asked to read it completely. After the subjects' finish reading, they are asked if they have read and understood the conditions outlined in the consent form. If they agree then they will be asked to fill out the details in the subject form and the voucher for the gift card. All the details provided by the participants will be kept confidential.

In this experiment we first ask the participant to be seated in a chair in front of the robot. Then they are asked to place their right hand on the robot handle and move it between the designated places over a period of approximately 1 second. During these trials we ask the participants to keep their eyes closed and will be asked to keep their hand in a relaxed position on the force manipulator. Also, the participants will be asked to keep their posture upright for all the trials. A trial can be moving the robot handle between the two lines inside a workspace or maintaining the arm posture inside a workspace. A total of 110 trials will be performed. The trials will be grouped into groups of 11 each. After every 11 trials the distance between the participant's arm and the force manipulator will be measured.

Each trial would consist of a motion of the force manipulator between two lines inside a workspace. Each trial is classified into 3 types of motion. The first 2 types of motions will be applied in a random manner, and the 3<sup>rd</sup> type of trial will be applied at the last. In the first type the participant will move the robot handle and there is no perturbation applied. In the second type the participant will experience a slight force in the direction perpendicular to the direction of their hand movement as they move the force manipulator between the two lines inside the workspace. In the third case the participant is asked to keep the robot handle inside the workspace. While they hold it and

maintain this position a force will be applied. The first 2 types of trials will happen in a random manner and the third type trial will happen at the last (the 11<sup>th</sup> trial). When the participants are supposed to carry out the third type of trial, we will let them know so that they can hold the manipulator inside the workspace.

**APPENDIX C.**

**MATLAB CODE FOR DATA PROCESSING**

```

clear all
close all
clc

% select the subject number (Sub) inside the excel worksheet that you want to
work on
Sub = 3;

% perturbation window size
win_size = 400; % 1 iteration = 1 msec

% iteration timing (sec)
t_stamp = 1/1000;

% butterworth filter with zero lag
fc = 40; % cutoff frequency (in Hz)
fs = 1000; % sampling frequency: LabVIEW while loop iteration (in Hz)
[par_1,par_2] = butter(2,fc/(fs/2), 'low');

%input Y if you have an excel sheet where you have stored the 2nd peak info
%and N if you don't and you are trying to look into velocity profile for
%recording that.
isVelFile = input('Does "velocity_2nd_peak_info" have 2nd peak information for
the subject data you are looking into?(Input Y/N): ', 's');
if isempty(isVelFile)
    reply = 'N';
end

%import velocity_1st_and_2nd_peak.xlsx
file_name = 'velocity_2nd_peak_info';
file_loc = ['./' file_name '.xlsx'];
[~,sheet_name]=xlsfinfo(file_loc);
peak_times = xlsread(file_loc,sheet_name{Sub});

%import all the files from folder "folder_name"
folder_name = ['Spring experiments data' '\' sheet_name{Sub}];
files = dir(['./' folder_name]);

sz = size(files,1);
mH = zeros(sz-2,1);
bH = zeros(sz-2,1);
kH = zeros(sz-2,1);
count = 0;
Rsqr = kH;
eqH = kH;

for i = 3:1:size(files)
    count = count+1;
    %% Extracting labview data
    if strcmpi(files(i).name((end-4):end),'.xlsx')
        % Import the Vicon data
        data_labview = xlsread([folder_name '\' files(i).name]);
    end
end

```

```

        % Rearranging the LabVIEW data
        labview.time = data_labview(2:end,1);           %time stamp between
sucessive data collection
        labview.force = data_labview(2:end,2:4);       %force data from
force/torque sensor
        labview.torque = data_labview(2:end,5:7);     %torque data from
force/torque sensor
        labview.theta1 = data_labview(2:end,8);       %theta_1 in robot
coordinate system
        labview.theta2 = data_labview(2:end,9);       %theta_2 in robot
coordinate system
        labview.beta = data_labview(2:end,10);        %beta
        labview.Case = data_labview(2:end,11);        %Instant when force
perturbation is applied
        clear data_labview
    end

%     trial_str = files(i).name;
%     trial_num = str2double(trial_str(15:16));
%     if (trial_num == 11)|| (trial_num == 12)|| (trial_num == 13)|| (trial_num
== 14)|| (trial_num == 15)
%         clearvars -except i count files folder_name peak_times t_stamp
win_size par_1 par_2 isVelFile...
%         mH bH kH Rsqr eqH
%         continue
%     end

% Filtering the data using ButterWorth filter with zero lag
labview.beta = filtfilt(par_1, par_2, labview.beta);
labview.force = filtfilt(par_1, par_2, labview.force);
labview.theta1 = filtfilt(par_1, par_2, labview.theta1);
labview.theta2 = filtfilt(par_1, par_2, labview.theta2);

angle = labview.beta+pi/1.8; % transforming rotational angle
F = (labview.force(:,1:2))'; % extracting just x, and y force

% rotating force from sensor axis to robot axis
parfor pk = 1:length(angle)
    matrix = [cos(angle(pk)) sin(angle(pk)); -sin(angle(pk))
cos(angle(pk))]; %rotation matrix
    rotatedF(:,pk) = matrix*F(:,pk);
end

%decimate force data
Fx = rotatedF(1,:); %force in X
Fy = rotatedF(2,:); %force in Y

C = forward(labview.theta1, labview.theta2);
Cy = C(:, 2);

%find point where perturbation was initiated
perPoint = ceil(find(labview.Case == 2));

%% specify the hand position with respect to the position of motor 1

```

```

win = 101; % the window to average for finding parameters at onset of
perturbation

d = Cy(perPoint-win:perPoint);
v = diff(d)/t_stamp;
a = diff(v)/t_stamp;
d_0 = mean(d);
v_0 = mean(v);
a_0 = mean(a);

finY = Cy(perPoint+1:perPoint+win_size);

%   plot(Fy(perPoint:perPoint+win_size))
%   pause

%% obtain force with respect to the equilibrium point
f_0 = mean(Fy(perPoint-win:perPoint));
Fy_diff = (Fy(perPoint+1:perPoint+win_size) - f_0).';

%% calculate the velocity and acceleration
vel = diff(finY)/t_stamp;
acc = (diff(vel))/t_stamp;

coeff_mH = acc-a_0;
coeff_bH = vel-v_0;
coeff_kH = finY-d_0;

force = Fy_diff;

fprintf('\n')
display(files(i).name)

% if peak values are already stored in excel sheet, retrieve it
% or else find the peak value
if isVelFile == 'Y'
    data_start = 1;
    data_end = peak_times(count,3);

    %figure(500+count);
    %plot(vel)
    %hold on; xline(data_end, 'r--', 'LineWidth', 0.5); hold off
    %title('Velocity (m/sec)','Interpreter', 'none')
%   pause
    %close (500+count) %close the figure by passing its figure number
else
    figure(500+count);
    plot(vel)
    title('Velocity (m/sec)','Interpreter', 'none')

```

```

disp('Please get the position of second peak from velocity graph and
record it in the excel sheet, then PRESS ENTER !!')

pause;
close (500+count) %close the figure by passing its figure number
continue
end

%% Multiple linear regression
%{
Here we apply a linear regression model in a window of data between the
first peak and the second peak in the velocity plot.

Let's assume the human arm model to follow the following equation:
 $F - F_0 = M(ddy-ddy_0) + C(dy-dy_0) + K(y - y_0)$  %y_0 is the instant right
before the onset of the perturbation

the equation is represented as follows;
y(:,4) = a(1)*y(:,1)+ a(2)*y(:,2) + a(3)*y(:,3)
%}

%% using fitlm function (without intercept)
tab_data = table(coeff_mH(data_start:data_end),
coeff_bH(data_start:data_end), coeff_kH(data_start:data_end), ...
force(data_start:data_end), 'VariableNames',{'ddot_x - ddot_x0',
'dot_x - dot_x0', 'x -x0', 'F-F_0 (N)'});

mdl = fitlm(tab_data,'Intercept',false); %using fitlm function with
intercept

mH(count,1) = table2array(mdl.Coefficients(1,1));
bH(count,1) = table2array(mdl.Coefficients(2,1));
kH(count,1) = table2array(mdl.Coefficients(3,1));

Rsqr(count,1)= mdl.Rsquared.Ordinary;

% Rsqr_custom(count,1) = Rsqrd(Fobs_ft, Fpre_ft);

%% calculate the equilibrium position of the hand
%{
f_0 = mH ddy_0 + bH dy_0 + kH yH
%yH is the hand displacement from hand equilibrium point
%}
eqY = (f_0 - mH(count,1)*a_0 - bH(count,1)*v_0)/kH(count,1);
eqH_robFrame = d_0 - eqY;
eqH(count,1) = eqH_robFrame - (-0.095-0.075); % w.r.t the center of the
workspace
%% clear variables except clearvars -except i count files folder_name
peak_times t_stamp win_size par_1 par_2 isVelFile...
mH bH kH Rsqr eqH
end

```

## BIBLIOGRAPHY

- [1] S. Haddadin, A. Albu-Schäffer, G. Hirzinger, “Safe Physical Human-Robot Interaction: Measurements, Analysis and New Insights”. In: Kaneko, M., Nakamura, Y. (eds) *Robotics Research. Springer Tracts in Advanced Robotics*, vol 66, 2010.
- [2] R. Alami et al., “Safe and dependable physical Human-Robot Interaction in anthropic domains: State of art and challenges,” *2006 IEEE/RSJ International Conference on Intelligent Robots and Systems*, Beijing, China, 2006, pp.1-16.
- [3] Daniel Sidobre, Xavier Broquère, Jim Mainprice, Ernesto Burattini, Alberto Finzi, Silvia Rossi, and Mariacarla Staffa, “Human-Robot Interaction,” *Springer Tracts in Advanced Robotics: Advanced bimanual manipulation*, Vol 80, 2012.
- [4] F. Sylos-Labini, A. d’Avella, F. Lacquaniti, and Y. Ivanenko, “Human-human interaction forces and interlimb coordination during side-by-side walking with hand contact”. *Frontiers in physiology*, 9, March, 2018, p. 179.E
- [5] A. Q. Keemink, H. van der Kooij, and A. H. Stienen, “Admittance control for physical human–robot interaction.” *The International Journal of Robotics Research*. 2018;37(11), pp. 1421-1444
- [6] S. Regmi, D. Burns, and Y. S. Song, “Humans modulate arm stiffness to facilitate motor communication during overground physical human-robot interaction,” *Scientific Reports*, 12(1), 2022.
- [7] G. L. Holmes, K. M. Bonnett, A. Costa, D. Burns and Y. S. Song, "Guiding a Human Follower with Interaction Forces: Implications on Physical Human-Robot Interaction," *2022 9th IEEE RAS/EMBS International Conference for Biomedical Robotics and Biomechatronics (BioRob)*, Seoul, Korea, 2022, pp. 1-6.
- [8] M. Wu, L. Drnach, S. M. Bong, Y. S. Song, and L. H. Ting, “Human-Human Hand Interactions Aid Balance During Walking by Haptic Communication,” *Frontiers in Robotics and AI*, 2021.
- [9] Buzzi J, Ferrigno G, Jansma JM and De Momi E (2017) On the Value of Estimating Human Arm Stiffness during Virtual Teleoperation with Robotic Manipulators. *Front. Neurosci.* 11:528
- [10] H. Gomi and M. Kawato, “Human arm stiffness and equilibrium-point trajectory during multi-joint movement.” *Biol Cybern.* 1997 Mar;76(3), pp.163-71.

- [11] T. Flash and F. A. Mussa-Ivaldi, "Human arm stiffness characteristics during the maintenance of posture," *Experimental Brain Research*, 82(2), 1990, pp. 315–326.
- [12] R. D. Trumbower, M. A. Krutky, B. S. Yang, and E. J. Perreault, "Use of self-selected postures to regulate multi-joint stiffness during unconstrained tasks," *PLoS ONE*, 2009;4(5):e5411.
- [13] S. Regmi, D. Burns, and Y. S. Song, "A robot for overground physical human-robot interaction experiments," *PLoS ONE* 17(11), 2022.
- [14] S. Regmi and Y. S. Song, "Design Methodology for Robotic Manipulator for Overground Physical Interaction Tasks". *Journal of Mechanism and Robotics*, 12(4), August 2020, p. 041002.
- [15] F. Rashid, D. Burns, and Y. S. Song, "Factors affecting the sensitivity to small interaction forces in humans," *2021 43rd Annual International Conference of the IEEE Engineering in Medicine & Biology Society (EMBC)*, 2021, pp. 6066-6069.
- [16] F. Rashid, D. Burns, and Y. S. Song, "Sensing small interaction forces through proprioception," *Scientific Reports*, 11(1), 2021, pp. 1-10.
- [17] N. Stefanov, A. Peer and M. Buss, "Role determination in human-human interaction," *World Haptics 2009 - Third Joint EuroHaptics conference and Symposium on Haptic Interfaces for Virtual Environment and Teleoperator Systems*, pp. 51-56.

## VITA

Tarani Kanth Kamma did his Bachelor of Engineering from GITAM University in the year 2007. He received his Master of Science in Manufacturing Systems from Southern Illinois University, Carbondale in the year 2010. He has obtained Lean Six Sigma Black Belt certification and Quality Process Analyst Certification from American Society of Quality (ASQ). He has done several internships in the field of process improvement and has gained several experiences in the area of Lean Manufacturing.

Prior to joining Missouri S&T, he was an Assistant Professor of Mechanical Engineering at Vignan college of Engineering where he taught Engineering Drawing and Engineering Mechanics. During this period, he has introduced several new courses based on Outcome Based Education (OBE). He has published 3 papers in various conferences, 2 of them in IEEE EMBS and in IEEE IEOM Proceedings.

While pursuing his master's at Missouri S&T, he has also worked as an intern at Gardner Denver where he successfully executed several projects which resulted in the company saving a lot of Scrap cost. He earned his Master of Science in Mechanical Engineering from Missouri University of Science and Technology, Rolla in May 2024.